Virulence

ISSN: 2150-5594 (Print) 2150-5608 (Online) Journal homepage: www.tandfonline.com/journals/kvir20

Genome-wide Identification of conditionally essential genes supporting *Streptococcus suis* growth in serum and cerebrospinal fluid

Maria Juanpere-Borras, Tiantong Zhao , Jos Boekhorst, Blanca Fernandez-Ciruelos, Rajrita Sanyal , Nissa Arifa , Troy Wagenaar , Peter van Baarlen & Jerry M. Wells

To cite this article: Maria Juanpere-Borras, Tiantong Zhao , Jos Boekhorst, Blanca Fernandez-Ciruelos, Rajrita Sanyal , Nissa Arifa , Troy Wagenaar , Peter van Baarlen & Jerry M. Wells (2026) Genome-wide Identification of conditionally essential genes supporting *Streptococcus suis* growth in serum and cerebrospinal fluid, Virulence, 17:1, 2600145, DOI: 10.1080/21505594.2025.2600145

To link to this article: https://doi.org/10.1080/21505594.2025.2600145

VIRULENCE
2026, VOL. 17, NO. 1, 2600145
https://doi.org/10.1080/21505594.2025.2600145

Taylor & Francis
Taylor & Francis Group

PATHOGEN GENOMICS

OPEN ACCESS Check for updates

Genome-wide Identification of conditionally essential genes supporting *Streptococcus suis* growth in serum and cerebrospinal fluid

Maria Juanpere-Borras [a], Tiantong Zhao[a], Jos Boekhorst [a], Blanca Fernandez-Ciruelos [a], Rajrita Sanyal[a], Nissa Arifa[a,b], Troy Wagenaar[a], Peter van Baarlen [a], and Jerry M. Wells[a]

[a]Host-Microbe Interactomics Group, Wageningen University and Research, Wageningen, Netherlands; [b]Research Center for Genetic Engineering, National Research and Innovation Agency (BRIN), Bogor, Indonesia

ABSTRACT

Streptococcus suis is a major cause of sepsis and meningitis in pigs, and zoonosis through the emergence of disease-associated lineages. The ability of *S. suis* to adapt and survive in host environments, such as blood and cerebrospinal fluid (CSF), is important for pathogenesis. Here, we used Transposon Sequencing (Tn-seq) coupled with Nanopore sequencing to identify conditionally essential genes (CEGs) for the growth of *S. suis* P1/7 in active porcine serum (APS) and CSF derived from choroid plexus organoids. To our knowledge, this is the first successful application of ONT to Tn-library screening, enabling rapid local runs and a publicly available analysis pipeline. Through comparative fitness analyses, we identified 33 CEGs that support growth in APS and 25 CEGs in CSF. These genes highlight the importance of pathways related to amino acid transport, nucleotide metabolism, and cell envelope integrity. Notably, the LiaFSR regulatory system and multiple ABC transporters were important for proliferation. We also identified several genes of unknown function as essential for growth, pointing to previously unrecognized genetic factors involved in *S. suis* adaptation during infection. These findings provide new insights into the genetic requirements for *S. suis* survival in host-like environments and a deeper understanding of its ability to adapt to distinct physiological niches.

ARTICLE HISTORY
Received 26 June 2025
Revised 7 October 2025
Accepted 2 December 2025

KEYWORDS
Streptococcus suis; pathogenesis; transposon library; nanopore sequencing; active porcine serum; cerebrospinal fluid

Introduction

Streptococcus suis (*S. suis*) is an encapsulated Gram-positive coccus that causes infections of the porcine respiratory tract, as well as severe invasive infections such as septicemia, arthritis, and meningitis [2,3]. Diseases caused by *S. suis* result in significant economic losses in the pork industry due to mortality, antimicrobial treatments, and the use of autogenous vaccines [4]. *S. suis* is also a public health concern for persons encountering diseased pigs or raw pork products due to the high zoonotic potential of specific lineages [5–7]. Highest cases of *S. suis* zoonotic disease occur in Southeast Asia, with Vietnam having the highest number of cases [8]. Currently, 29 virulence-associated serotypes of *S. suis* have been reported, with serotype 2 being the most common cause of invasive disease in swine and human infections [6,7].

Asymptomatic carriage of *S. suis* in the upper respiratory, genital, and intestinal tracts of pigs is common [9]. *S. suis* exhibits relatively low invasiveness toward epithelial cells supporting the hypothesis that the main route of entry into the body is via the palatine tonsils [10,11]. Immunohistochemistry research shows that *S. suis* can enter deep in the tonsillar crypts, where the surface epithelium becomes a single-cell layer thick, facilitating bacterial uptake and translocation [12]. One hypothesis is that *S. suis* is phagocytosed, but not killed, by specific subsets of tonsillar macrophages, allowing phagocytosed *S. suis* bacteria to replicate and travel through the efferent lymphatics to the bloodstream or directly enter the circulation via the blood vessels in the lymphoid tissue [13,14]. Once in the bloodstream, *S. suis* can cause sepsis, and meningitis upon crossing the blood–brain barrier or the blood-cerebrospinal fluid barrier [2,15]. The precise pathways and molecular mechanisms enabling *S. suis* to infect hosts remain poorly characterized [16]. This underscores the need for further studies to delineate the genetic and cellular factors underpinning *S. suis* pathogenesis [16].

Despite advances in understanding the pathogenesis of *S. suis*, the development of effective vaccines remains challenging. This difficulty arises from the extensive genetic diversity of *S. suis* [3], and the fact that similar virulence functions can be carried out by different genes across pathogenic lineages [17,18]. Virulence factors recognized to play important roles in *S. suis* pathogenesis are the cytotoxin suilysin, the capsular

CONTACT Jerry M. Wells jerry.wells@wur.nl; Maria Juanpere-Borras maria.juanpereborras@wur.nl
Supplemental data for this article can be accessed online at https://doi.org/10.1080/21505594.2025.2600145

polysaccharide, and enolase [19,20]. Surface-exposed enolase of *S. suis* hijacks the host plasminogen-plasmin proteolytic system to break down the host extracellular matrix [19–21].

Beyond classical virulence factors, genes that enable stress resistance, metal homeostasis, and adaptation to host environments are also crucial for *S. suis* pathogenesis [15,22]. To colonize the host, survive, and replicate during host infection, *S. suis* must compete with other microorganisms for scarce nutrients and adapt to changes in pH and oxygen levels [22]. Bacterial sensory systems play a crucial role in detecting and responding to environmental changes, nutrient availability, and rapidly regulating gene expression to support replication, which is crucial for pathogenesis and transmission. Hence, identifying conditionally essential genes (CEGs) will uncover the genetic basis of metabolic adaptation of *S. suis* across host niches, deepen understanding of pathobiology, and potentially identify targets for new therapeutic strategies [23]. In *Streptococcus pneumoniae (S. pneumoniae), in vivo* studies in CSF during experimental meningitis identified dozens of genes required for replication, capsule synthesis, and metabolic adaptation [24]. Similarly, CEGs involved in carbohydrate metabolism, metal homeostasis, and cell envelope were identified in studies on *Klebsiella pneumoniae* in human serum [25]. Together, these findings underscore that identifying CEGs for the growth of bacterial pathogens in host environments expands opportunities for therapeutic intervention.

A substantial portion of the *S. suis* genome has hitherto remained uncharacterized, with numerous genes encoding hypothetical proteins with unknown functions, as described in NCBI databases (NC_012925). Consequently, critical genes for infection and pathogenesis may have remained undiscovered. To address this, unbiased genome-wide screening methods are necessary to identify annotated and hypothetical genes necessary for *S. suis* replication and survival in the host.

In this study, we used Transposon Sequencing (Tn-seq), a next-generation sequencing technique to identify genes involved in *S. suis* growth and survival in active porcine serum (APS) and cerebrospinal fluid (CSF) extracted from the lumen of iPSC-derived choroid plexus (ChP) organoids [1]. CSF within the lumen of 30–40-d-old human ChP organoids closely resembles *in vivo* CSF [26]. The ChP organoid model offers an alternative approach to extracting CSF from animals or humans. Significant differences in metabolite concentrations have been measured between CSF and serum [27]. The latter study, conducted on 58 healthy control individuals, showed that methionine, glutamic acid, and glycine were only detected in a small number of CSF samples but were present in nearly all serum samples. Additionally, inosine was exclusively detected in CSF samples, likely due to its critical roles in purine and energy metabolism and in neuroprotection, where it supports neural repair, and reduces oxidative stress [27,28]. Tn-seq provides a non-biased, systematic approach by utilizing a saturated transposon insertion library (Tn-library) [29]. The Tn-seq procedure has been recently used in *S. suis* S10, to identify genes involved in pathogenesis. Using an *in vivo* model, bacteria were inoculated intrathecally in pigs, and mutants were recovered from different body fluids [30]. That *in vivo* work provides a valuable reference for niche-specific fitness in the natural host. In contrast, our study profiles CEGs *ex vivo*, which avoids animal use and reduces *in vivo* bottlenecks, providing a complementary dataset for pathway level comparison. In this study, a Tn-library was generated in *S. suis* P1/7, a zoonotic serotype 2 strain [16,22] which was cultured under both control and test conditions. By sequencing the flanking regions of transposon insertions and comparing their frequencies between conditions, we identified insertions that either enhanced or impaired bacterial fitness [29]. To sequence Tn-libraries in-house with rapid turnaround and accuracy, we used Oxford Nanopore sequencing technology. To validate the functional role of specific genes, we performed bioassays using chemically defined media (CDM), APS, and CSF to assay proliferation capacities of *S. suis* gene-specific deletion mutants.

Our high-throughput screening results revealed the critical role of specific metabolic pathways for *S. suis* P1/7 growth in APS and CSF. Nucleotide metabolism was essential for survival and proliferation in APS, while amino acid uptake was critical for proliferation in CSF. We also characterized a so far unknown nucleotide ABC transporter in *S. suis*, essential for purine uptake. Furthermore, our analysis discovered that the LiaFSR three component system and several other uncharacterized genes appear to be involved in *S. suis* pathogenesis. Notably, we demonstrated, for the first time, the feasibility of using CSF extracted from ChP organoids as a model system. A preliminary version of this manuscript was posted as a preprint on bioRxiv [31]

Materials and methods

Bacterial strains and growth conditions

Streptococcus suis strain P1/7 (ATCC, BAA-853) [32] was cultured in Todd-Hewitt medium (Thermo Fisher

Scientific™, CM0189) supplemented with 0,2% of yeast extract (Thermo Fisher Scientific™, 212,750) (THY) at 37°C with 5% CO_2. High transformation-efficiency *Escherichia coli* strain Top10 (Thermo Fisher Scientific™, C404010) was cultured in LB medium (Merck, 1,102,850,500) at 37°C with vigorous shaking. Chloramphenicol (Sigma-Aldrich, C0378-25 G) was added to the media at a final concentration of 5 µg/mL for *S. suis* and 20 µg/mL for *E. coli*.

Growth measurements

Growth of *S. suis* WT and deletion mutants in THY were measured by absorbance (OD_{600}) every hour for 8 hr. Growth measurements in APS and CSF were performed hourly by making serial dilutions in PBS and plating on agar plates to obtain CFU/mL. For all strains, overnight cultures were first pelleted at 6000 rpm for 5 min, and pellets were resuspended in PBS. The appropriate volume of bacterial culture was inoculated into APS or CSF to achieve an OD_{600} of 0.015. For THY growth measurements, bacterial overnight cultures were directly inoculated without prior pelleting and resuspension in PBS. THY growth curves were performed in two independent experiments with three biological replicates. APS and CSF growth curves were performed in two independent experiments, with three biological replicates per experiment and two technical replicates per biological replicate. For mutants that did not reproduce a phenotype, assays were run once to conserve limited APS/CSF volumes. Δ*liaS* was assayed in one independent experiment due to limited material from that APS batch; Δ*liaR* (same operon) was tested in two independent experiments and showed concordant behavior. For additional validation, Δ*purA*, ΔSSU_RS04755, and ΔSSU_RS09155 were each tested using a second, independently constructed deletion mutant generated with a non-overlapping CRISPR guide (data not shown).

Growth curves in chemically defined media

The complete list of basic components and stock solutions used to prepare CDM is found in supplementary materials Table S1. For the preparation of 2 mL of CDM, the following constituents were used: 450 µL of CDM buffer, 200 µL amino acids mix, 200 µL of glucose, 20 µL of pyruvate, 20 µL of vitamins mix, 20 µL of metal mix, 4 µL of manganese solution, and 2 µL of choline chloride solution. Nucleobases were added at the final concentrations ranging from 1 to 100 mg/L, and the mixture was brought to 2.00 mL with sterile water. Subsequently, 200 µL of CDM was added to each well of a 96-well plate along with 2 µL of THY overnight cultures. OD_{600} readings were obtained using a SpectraMax® M3 Multi-Mode Microplate Reader (Avantor, Radnor, PA, USA) at 37°C. Growth-curve assays were performed in at least two independent experiments, each with three biological replicates. For ΔSSU_RS04755, two independent deletion mutants generated with non-overlapping CRISPR guides were used in the assays.

Transposon vector cloning

The materials and protocols for constructing the transposon library were provided by Tim Van Opijnen's lab (Tufts University School of Medicine, Boston, Massachusetts) and modified as described below [33]. *Magellan6* encodes spectinomycin resistance between two inverted repeat sequences [33]. Given that *S. suis* has intrinsic resistance to spectinomycin, we engineered the *Magellan6* plasmid such that the Himar1 *mariner* transposon carried a chloramphenicol resistance gene under the control of the P32 promoter. The plasmid containing the Himar1 *mariner* transposon, *Magellan6*, was purified using the Qiagen Miniprep kit (QIAprep Spin Miniprep Kit, 27,106), following the manufacturer's recommendations. Linearization of the plasmid was performed using the restriction enzymes FastDigest *Sma*I and *Swa*I (Thermo Fisher Scientific™, 10,324,630, and 15,390,291). A DNA fragment containing the P32 promoter and chloramphenicol acetyltransferase resistance gene was amplified by PCR using primers P001 and P002 (Table S2), and the high-fidelity Q5 polymerase (NEB, M0493S), using plasmid pLABTarget as a template [34]. The DNA fragments were ligated together using Hifi Assembly (NEB, E2621S), to generate plasmid Meg6SS that now encoded Himar1 *mariner* transposon with the desired chloramphenicol resistance gene.

Generation of Tn-library for S. suis P1/7

Genomic DNA (gDNA) and plasmid DNA solutions were concentrated using a SpeedVac (Thermo Fisher Scientific™, RVT5105) until they reached a concentration of at least 350 ng/µL. 36 µL of purified C9T transposase was mixed with 4 µg of gDNA and 4 µg of plasmid and incubated at 30°C for 6 hr. DNA fragments containing the transposon were transformed into *S. suis* using the natural competence method described by Zaccaria et al. [35]. Briefly, 10 µL aliquots of treated DNA were combined with 5 µL of competence inducer peptide ComS and 100 µL of *S. suis* THY culture at OD_{600} values between 0.035 and 0.05. After

2-hr incubation, aliquots were pooled to a final volume of approximately 900 µL. A 1/10 dilution of 10 µL of the mixture was plated on THY chloramphenicol agar plates for CFU counting and the remaining 900 µl centrifuged at 6000 rpm for 5 min. Then, 800 µL of supernatant was removed and the pellet resuspended in the remaining 100 µL before plating on THY agar plates containing 5 µg/mL chloramphenicol. This process was repeated four times, resulting in 4 libraries with colony counts of approximately 10K, 1.5K, 3.3K, and <1K, respectively.

Generation of choroid plexus organoids and extraction of cerebrospinal fluid

Six-well plates (Corning, 07–200–83) were pre-coated with Vitronectin (STEMCELL, 07180) in CellAdhere™ Dilution Buffer (STEMCELL, 07183) at room temperature for 1 hr. Human iPSC line EDi002-A (EBiSC™) were maintained on vitronectin-coated 6-well plates in mTeSR1 (STEMCELL, 85,857). Media were changed daily, and cells were passaged once a week. ChP organoids were generated using the STEMdiff™ Choroid Plexus Organoid Differentiation Kit (STEMCELL, 100–0824) and the STEMdiff™ Choroid Plexus Organoid Maturation Kit (STEMCELL, 100–0825), following previous protocols with minor modifications [36]. Briefly, iPSC were dissociated into single-cell suspensions using Accutase (STEMCELL, 07920). On day 1, 1×10^5 cells were seeded into a well of Corning® 96-well round-bottom ultra-low attachment microplate (Corning, 7007) in 100 µL of embryoid body (EB) Formation Medium and 10 µM Y-27632 (ROCK inhibitor; STEMCELL, 72,302). On day 2 and day 4, fresh 100 µL of EB Formation Medium was added to each well. EBs with diameters ranging between 400 and 600 µm were typically observed on day 5 at which time EB Formation Medium was replaced with 200 µL/well of Induction Medium. On day 7, each EB was embedded in 15 µL of Matrigel® (Corning, 734–1101) dropwise on sheets of parafilm and incubated at 37 °C for 30 min to polymerize Matrigel® (16 EB per sheet of parafilm). The sheets of parafilm were each positioned above one well of a 6-well ultra-low adherent plate (STEMCELL, 100–0083) using sterile forceps. All 16 Matrigel® droplets were gently washed off sheets and put into one well using 3 mL of Expansion Medium. Each 6-well plate was shaken back and forth three times to ensure even distribution of EB and incubated at 37 °C for 3 days. On day 10 the Expansion Medium was carefully replaced with 3 mL/well of Choroid Plexus Differentiation Medium, and plates were placed on a platform rotator (Fisherbrand™, 15,504,080) in the incubator. On day 13, Choroid Plexus Differentiation Medium was refreshed. From day 15, Choroid Plexus Differentiation Medium was replaced with 3 mL/well Maturation Medium and renewed every 3 d. By day 30, ChP organoids epithelia resemble cyst-like structures filled with CSF-like fluid. ChP organoids between day 30 to day 40 were used to harvest CSF from the organoid lumen using a 0.30 × 12 mm BL/LB needle attached to a 1 mL syringe.

Transposon library screening

For APS screening, 60 µL of *S. suis* Tn-library were inoculated into 10 ml pre-warmed THY broth or APS (Thermo Fisher Scientific™, 26,250,084), with two biological replicates for each condition and incubated for 5 hr at 37°C with 5% CO_2. For CSF screening, 250 µL of Tn-library stock was thawed in 10 ml of THY medium and cultured for 3.5 hr until it reached concentration of 5×10^8 CFU/mL, and then centrifuged and resuspended in 10 ml of PBS. Then 100 µL of the enriched Tn-library in PBS (Fisher Scientific, 10,769,033) was inoculated in 10 ml of THY and 10 ml of CSF in triplicates and cultured at 37°C with 5% CO_2 until cultures reached an OD_{600} of 0.6. Cultures were centrifuged at 4000 rpm for 10 min, the supernatant discarded, and the bacterial pellets stored at – 20 degrees until further use. DNA was extracted from bacterial pellets using DNeasy PowerSoil kit (Qiagen, 47,016) following the manufacturer's recommendations.

Sample preparation

After library growth under the different conditions (APS, CSF, and THY), bacterial DNA was isolated and processed as described by Van Opijnen & Camilli [33] Briefly, approximately 2 µg of genomic DNA was digested with the *MmeI* restriction enzyme (NEB, R0637L) and dephosphorylated using Quick CIP (calf intestinal alkaline phosphatase) (NEB, M0525S) to avoid re-ligation. The oligonucleotide primers incorporating the adapter sequences (P003 and P004, Table S2), were annealed by mixing equimolar concentrations of each primer in water in 1.5 ml Eppendorf tubes, heating the tubes to 96°C for 3 min, and gradually cooling the tubes to room temperature. Phosphorylated adapters were ligated to the overhangs generated by digestion of bacterial DNA with *MmeI*, using T4 DNA ligase (NEB, M0202S). After adapters ligation, transposon-containing fragments of bacterial DNA were amplified by PCR. The forward primer annealed to the inverted repeat sequence that is present

at each end of the transposon, while the reverse primer annealed to the ligated adapter (P005 and P006, Table S2). The PCR reaction included 2 µL of the ligation mix and High-fidelity Q5 polymerase (NEB, M0493S) for 35 cycles. Total volumes of PCR reactions were loaded onto 0.8% agarose gel, and bands corresponding to 150-180 base pairs (bp) that were expected to contain transposon-enriched fragments were excised and purified using Invisorb fragment cleanup kit (Invitek molecular, 1,020,300,300) (Figure 1).

Library sequencing with nanopore

PCR amplicons were prepared and barcoded for sequencing following the manufacturer's instructions using the native barcoding kit (ONT, SQK-NBD112. 24), the ligation sequencing kit (ONT, SQK-LSK112) kit, and flow cells (ONT, FLO-MIN106D) on MinION Mk1c and Mk1b (ONT, Oxford, United Kingdom) sequencing devices; device outputs were handled using MinKNOW software (version 23.07.15). Sequencing ran until all reads were sequenced (approximately 24 hr). The resulting FAST5 files, containing raw nanopore data of each sample, were converted to FASTQ files via basecalling (Guppy version 7.1.4).

Analysis of Tn-seq data

For nanopore reads sequence analysis (Figure 1), we filtered reads to include those within the expected size range of our PCR amplicon, roughly 150 to 180 bp. Subsequently, we conducted a two-step screening process for the 20 bp of transposon sequence upstream of the transposon insertion site so that only reads containing the forward transposon (Tn) sequence (ACTTATCATCCAACCTGTTA) or the reverse Tn sequence (TAACAGGTTGGATGATAAGT) were retained for further analysis. For the filtered reads, only the 14 bp immediately adjacent to the respective forward or reverse Tn sequences were selected for alignment to the *S. suis* P1/7 reference genome using Bowtie2. Only reads with 100% identity to a single gene fragment were retained; reads that mapped to more than one gene in the genome were discarded. The number of reads per TA site was quantified, and the data was compiled into a Wiggle (WIG) file. TA sites

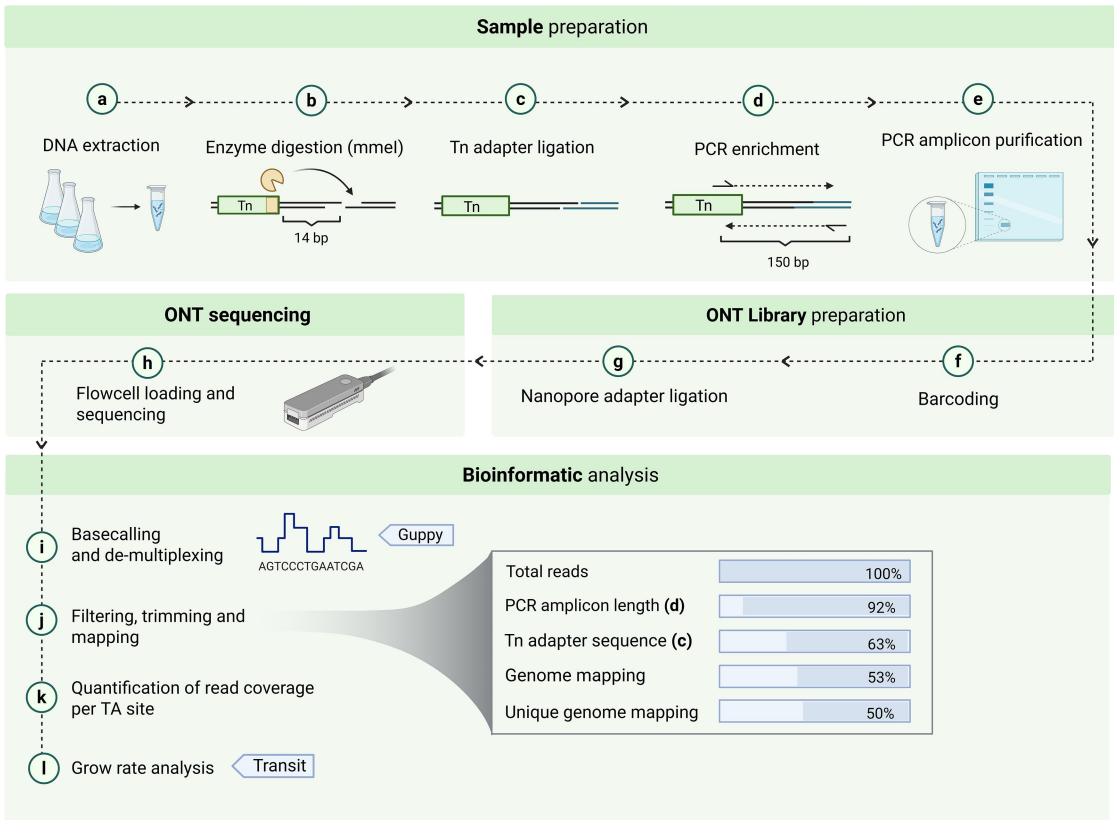

Figure 1. Workflow for Tn-seq sample processing, sequencing, and bioinformatic analysis. (a-e) Sample preparation begins with DNA extraction, followed by enzyme digestion with MmeI, Tn adapter ligation, PCR enrichment, and amplicon purification. (f-h) Ont library sequencing. (i-l) *in-silico* processing of sequencing output and data analysis. (steps j and k were specifically developed for this study).

with zero insertions (no matches) were also included in the WIG file during harmonization to ensure the data includes all TA sites per gene, for calculation and comparison during the fold-change analysis. The harmonized WIG files from each replicate were assessed for library quality using the Transit "tnseq_stats" module (version 3.2.7). This analysis provided metrics such as library saturation at TA sites, total mapped reads, and insertion count distributions. For CEGs analysis, the harmonized wig files from each replicate of both the control and test conditions were used as input into Transit (version 3.2.7) for growth rate analysis using the Transit "resampling test" module with default parameters. Genes that exhibited a $\log_2$ Fold Change ($\log_2$FC)>1 and achieved statistical significance (adj. p-value <0.05) were compiled into a final list (Table 1). The set of filtered genes and encoded proteins were annotated by retrieving the corresponding gene descriptions and biological process annotations from NCBI and KEGG databases, respectively.

Gene deletion mutants

In frame deletion mutants were constructed using CRISPR/Cas9 based technology essentially as described by Gussak et [37]. Briefly, mutants were generated by transforming *S. suis* P1/7 with a gRNA-Cas9 co-expression plasmid (pSStarget) and a linear DNA repair template. Upon transformation, Cas9 endonuclease was expressed and directed by the co-expressed guide RNA to specific target gene, where Cas9 induced a double-stranded cut that was repaired by the *S. suis* homologous recombination machinery using the introduced DNA repair template. Resulting colonies were screened for gene-specific deletion mutants and site-specific mutant strains were cured from expression plasmids.

Three different 20 bp guide RNAs were designed for each target gene. Single-stranded oligonucleotides were designed using Benchling software, and synthesized by IDT Technologies. Each primer included a 4 bp overhang compatible with the overhangs of the linearized pSStarget plasmid (P007 to P048, Table S2). Equimolar concentrations of complementary primers for each guide were mixed with annealing buffer (10 mM Tris, pH 7.5, 50 mM NaCl, 1 mM EDTA) and annealed in a thermocycler (Bio-Rad, Hercules, CA, USA) (5 min at 95°C and gradually cooling to 25°C at 1°C/min). The empty pSStarget plasmid was linearized using the BsaI enzyme (NEB, R3733S) and purified Invisorb Fragment CleanUp kit (Invitek, 1,020,300,300). The annealed guide and digested plasmid were ligated using T4 DNA ligase (NEB, M0202S) for 1 hr at room temperature and subsequently incubated overnight at 4°C. The ligation mixture was transformed into chemically competent *E. coli* Top10 cells and plated on LB agar plates containing 10 µg/mL of chloramphenicol, followed by overnight incubation at 37°C. Colonies were screened for correct plasmid constructs using primers P077 and P078 (Table S2), and plasmids and guide were extracted from these colonies using the Qiagen Miniprep kit (QIAprep Spin Miniprep Kit, 27,106).

The repair template was constructed by amplifying approximately 1000 bp upstream and downstream of the target gene using primers (P049 to P076, Table S2). These primers were designed to include approximately the first and last 30 bp of the target gene, ensuring that the entire gene was not deleted to avoid potential polar effects on downstream genes. PCR products were subsequently ligated through Splicing by Overlap Extension (SOE) PCR using external primers, HA1_fwd_X, and HA2_rev_X (Table S1). After each PCR step, the PCR products were purified using the Invisorb Fragment CleanUp kit (Invitek, 1,020,300,300).

gRNA-Cas9 co-expression plasmids and repair templates were transformed into *S. suis* using the natural competence method described by Zaccaria et al. [35]. Briefly, 250 µL of an overnight culture of *S. suis* P1/7 WT were inoculated into 10 mL of THY broth and grown until the OD_{600} reached between 0.035 and 0.058. A 100 µL aliquot of *S. suis* P1/7 culture was combined with 5 µL of competence-inducing peptide ComS, 200–500 ng of plasmid DNA, and 1 µg of repair template. The mixture was incubated at 37 °C with 5% CO_2 for 2 hr and plated on THY agar plates containing 5 µg/mL of chloramphenicol. Colonies with the correct gene deletion were identified using PCR and external primers HA1_fwd_X and HA2_rev_X (Table S2), and these colonies were cured from plasmids by performing two consecutive overnight passages in THY medium without chloramphenicol, followed by phenotypic verification by loss of growth on THY with chloramphenicol.

In silico *amino acid sequence alignments and protein structure predictions*

Amino acid sequences were obtained from the *S. suis* P1/7 genome annotation in NCBI (nucleotide ID NC_012925) for SSU_RS04755 and from Uniprot for PnrA (A0A0H2UPF3) and TmpC (P29724). Multiple sequence alignment of the amino acid sequences of SSU_RS04755, PnrA, and TmpC were performed using the Clustal Omega algorithm integrated within Jalview (version 2.11.3.3) software, using default parameters. Structure prediction of

Table 1. List of CEGs, identified by Tn-seq, that were conditionally essential to support *S. suis* growth in APS and CSF compared to THY(adj. p-vale <0.05; $Log_2FC < -1$). Genes are ordered from lowest to highest log_2FC; genes belonging to the same operon are marked with the same symbol in the "Operons" column.

Locus tag	Name	Product	Main biological process	Operons	Log_2FC
Genes identified by tn-seq in APS					
SSU_RS08850	–	adenylosuccinate synthase	Purine metabolism		**-3,19**
SSU_RS00280	*purB*	adenylosuccinate lyase	Purine metabolism		**-2,84**
SSU_RS06600	–	ABC transporter permease	Transporter	□	**-2,28**
SSU_RS02595	*ppc*	phosphoenolpyruvate carboxylase	Carbon metabolism		**-1,86**
SSU_RS05280	*ptsP*	phosphoenolpyruvate–protein phosphotransferase	Transporter		**-1,85**
SSU_RS06605	*trpX*	tryptophan ABC transporter substrate-binding protein	Transporter	□	**-1,84**
SSU_RS04185	*guaA*	glutamine-hydrolyzing GMP synthase	Purine metabolism		**-1,77**
SSU_RS06595	–	ABC transporter ATP-binding protein	Transporter	□	**-1,73**
SSU_RS06820	–	bifunctional oligoribonuclease/PAP phosphatase NrnA	Sulfur metabolism		**-1,65**
SSU_RS09155	–	hypothetical protein	NI		**-1,65**
SSU_RS09655	–	LacI family DNA-binding transcriptional regulator	Transcription factor		**-1,58**
SSU_RS06385	–	acyl-ACP thioesterase domain-containing protein	NI		**-1,56**
SSU_RS06740	–	hypothetical protein	NI		**-1,53**
SSU_RS01575	–	Fur family transcriptional regulator	Transcriptional factor		**-1,43**
SSU_RS04755	–	BMP family protein	Transporter	●	**-1,34**
SSU_RS07155	–	YtxH domain-containing protein	NI		**-1,34**
SSU_RS05100	–	mannonate dehydratase	Carbohydrate metabolism		**-1,29**
SSU_RS02715	–	amino acid ABC transporter substrate-binding protein	Transporter	◊	**-1,26**
SSU_RS02080	*liaF*	cell wall-active antibiotics response protein LiaF	Signal transduction		**-1,21**
SSU_RS04655	*pta*	phosphate acetyltransferase	Carbon metabolism		**-1,18**
SSU_RS07195	–	hypothetical protein	NI		**-1,18**
SSU_RS06140	*tpx*	thiol peroxidase	Oxidoreductases		**-1,17**
SSU_RS09860	*guaB*	IMP dehydrogenase	Purine metabolism		**-1,17**
SSU_RS04750	–	ABC transporter ATP-binding protein	Transporter	●	**-1,15**
SSU_RS04745	–	ABC transporter permease	Transporter	●	**-1,14**
SSU_RS02750	–	DegV family protein	NI		**-1,11**
SSU_RS05325	–	LacI family DNA-binding transcriptional regulator	Transcriptional factor		**-1,11**
SSU_RS06410	–	arsenate reductase	Oxidoreductases		**-1,11**
SSU_RS06645	–	lactonase family protein	Carbon metabolism		**-1,1**
SSU_RS05710		glucosaminidase domain-containing protein			**-1,05**
SSU_RS04420	*pyrE*	orotate phosphoribosyltransferase	Pyrimidine metabolism		**-1,02**
SSU_RS04510		ABC transporter substrate-binding protein/permease	Transporter	◊	**-1,02**
SSU_RS06155	*tehB*	SAM-dependent methyltransferase TehB	Transferases		**-1,01**
Genes identidied by tn-seq in CSF					
SSU_RS02635	–	hypothetical protein	NI		**−3.22**
SSU_RS06605	*trpX*	tryptophan ABC transporter substrate-binding protein	Transporter	□	**−2.97**
SSU_RS06600	–	ABC transporter permease	Transporter	□	**−2.88**
SSU_RS01560	–	hypothetical protein	NI		**−2.78**
SSU_RS06595	–	ABC transporter ATP-binding protein	Transporter	□	**−2.63**
SSU_RS00910	*pgk*	Phosphoglycerate kinase	Carbohydrate metabolism		**−2.61**
SSU_RS02500	–	hypothetical protein	NI		**−2.61**
SSU_RS07925	*glyQ*	Glycine–tRNA ligase alpha subunit	Translation		**−2.55**
SSU_RS04515	*artM*	Arginine transport ATP-binding protein ArtM	Transporter		**−2.54**
SSU_RS06355	*mscL*	Large-conductance mechanosensitive channel	Signaling and cellular processes		**−2.41**
SSU_RS03420	*srlR*	Glucitol operon repressor	Transcriptional factor		**−2.17**
SSU_RS04835	*pstB3_1*	Phosphate import ATP-binding protein PstB	Transporter		**−2.13**
SSU_RS08105	*fabH*	3-oxoacyl-[acyl-carrier-protein] synthase 3	Lipid metabolism		**−1.85**
SSU_RS07155	–	hypothetical protein	NI		**−1.43**
SSU_RS06420	*rpiA*	Ribose-5-phosphate isomerase A	Carbohydrate metabolism		**−1.42**
SSU_RS04600	*lacR_2*	Lactose phosphotransferase system repressor	Transcriptional factor		**−1.38**
SSU_RS02705	*yecS_2*	L-cystine transport system permease protein YecS	Transporter	◊	**−1.3**
SSU_RS08470	*ilvH*	Putative acetolactate synthase small subunit	Carbohydrate metabolism		**−1.3**
SSU_RS02715	*fliY*	L-cystine-binding protein FliY	Transporter	◊	**−1.14**
SSU_RS03250	–	Phosphoglycerate dehydrogenase	Energy/Amino acid metabolism		**−1.1**
SSU_RS02710	*glnQ_2*	Glutamine transport ATP-binding protein GlnQ	Transporter	◊	**−1.08**
SSU_RS07955	*metQ*	putative D-methionine-binding lipoprotein MetQ	Transporter		**−1.03**
SSU_RS07855	–	hypothetical protein	NI		**−1.02**
SSU_RS03205	–	hypothetical protein	NI		**−1.01**
SSU_RS05450	–	hypothetical protein	NI		**−1**

SSU_RS04755 was performed using the SWISS-MODEL server (https://swissmodel.expasy.org). Structure alignment of the predicted protein encoded by SSU_RS04755 from *S. suis* and PnrA was performed using PyMOL (version 3.0.3).

Identification of promoter regions with putative LiaR binding boxes

Identification of promoter regions potentially containing a LiaR binding box was performed using the FIMO tool from the MEME suite (https://meme-suite.org/

meme/tools/fimo) [38], utilizing the LiaR binding box motif identified from *Bacillus subtilis* as input [39]. The resulting list of genes was manually curated to retain only sequences with p-value <0.05 and located within 200 bp upstream of a gene. This analysis identified 48 genes with a putative LiaR binding box in their promoter regions (Table S3).

Analysis of differential gene expression by qPCR

S. suis P1/7 and *S. suis* Δ*liaR* mutant were grown to exponential phase (approximately OD_{600} 0.3) in THY broth at 37°C with 0.5% CO_2. A 10 ml aliquot was pelleted by centrifugation at 4000 rpm for 10 min, the supernatant was discarded, and the pellet snap-frozen in liquid nitrogen before being stored at − 80°C overnight. RNA was extracted from the pelleted cells using the RNeasy Mini Kit (Qiagen, 74,104) following the manufacturer's instructions with specific modifications. Pellets were resuspended in 700 µL of RLT buffer containing 0.1% β-mercaptoethanol and transferred to lysing matrix B 2 mL tubes (MP Biomedicals, 6,911,100). Bacterial cells were lysed using a FastPrep-24™ 5 G bead beating grinder and lysis system (MP Biomedicals, Solon, OH, USA) with settings; 4.0 m/sec, All-MetalQuickprep adapter, 40 s. The tubes were centrifuged for 1 min at 10,000 rpm, and the supernatant was transferred to a clean Eppendorf tube. Subsequent steps were carried out using the manufacturer's protocol. Final RNA concentrations were measured using the Qubit RNA Broad Range Kit (Thermo Fisher Scientific™, Q10211) and a Qubit 4 fluorometer (Thermo Fisher Scientific™, Waltham, MA, USA). The Quantitect Reverse Transcriptase Kit (Qiagen, 205,311) was used for DNA deletion and cDNA synthesis, with 500 ng of RNA as input. For differential gene expression analysis, 96-well white PCR plates (Bio-Rad, ML9651) and GoTaq qPCR Master Mix (Promega, A6002) were used in a CFX96 Real-Time PCR System (Bio-Rad, Hercules, CA, USA). Primers for each gene are listed in Table S1 (from P079 to P086). Gene expression was calculated using the 2-ΔΔCt method relative to the reference gene *gyrA*. Statistical analysis was performed using GraphPad Prism v10.6.1. We applied an ordinary one-way ANOVA followed by Dunnett's multiple comparisons test, comparing each mutant to the WT control. Data are presented as mean ± standard deviation.

Results

Obtaining in vitro *Tn-libraries for S. suis P1/7*

The transposon library was constructed using a modified version of the Tn-Seq protocol optimized for *S. pneumoniae* and described by Tim van Opijnen et al. [29]. Using this optimized protocol, we obtained four libraries that were combined to obtain 1 single library of approximately 15K mutants. We evaluated library quality using the control libraries generated in THY medium, which served as the reference condition for subsequent essentiality comparisons. Across five replicates, saturation ranged from 44% to 67%, with total mapped read counts between 1.2 and 2.8 million. The distribution of insertion counts was highly skewed with heavy-tailed profiles, consistent with expectations for Himar1 libraries. In total, 91% of coding sequences contained at least one insertion, indicating broad representation of the genome. These results indicate that the THY control libraries provided sufficient coverage to support reliable identification of CEGs.

Development of a nanopore sequencing protocol for sequencing of the Tn-libraries

After culturing the Tn-library in test (APS or CSF) and control (laboratory culture medium THY) media, DNA was extracted and processed as outlined in Methods section to obtain a PCR amplicon suitable for sequencing. We opted for nanopore PCR amplicons sequencing to have an in-house method for amplicon sequencing and analysis that could be optimized when appropriate. As it was the first time nanopore technology had been used for this purpose, we designed an in-house pipeline for processing and analyzing the sequenced nanopore reads (Figure 1), which is available at (https://github.com/MariaJuanpereBorras/Nanopore-TnSeq-Pipeline). For each sample, i.e. each Tn-library aliquot cultured in test or control media, nanopore sequencing generated between 0.7 and 5.4 million reads, which were filtered to remove fragments larger or smaller than the expected length of the amplicon (around 180 bp), resulting in an average discard rate of 5%. In the subsequent step, reads were selected based on the presence of the transposon sequence (underlined region of P005, Table S2); 64% of the total reads were retained during this phase. After this step, reads were trimmed to retain only the 14 base pairs immediately adjacent to the transposon end sequence. When these 14 bp inserts were mapped to the *S. suis* P1/7 genome (NCBI accession no. NC_012925), 55% of the *de novo* sequenced reads had a perfect match, and 51% had a unique perfect match; the remaining 4% were discarded because they did not map to a unique genomic location. After running the harmonized wig files in Transit (version 3.2.7) [40], a final list detailing the increased or decreased log_2FC for each gene in the test condition compared to the control was generated. Filtering the data on negative

log_2FC (< −1) and adjusted p-value (< 0,05), we obtained a final list of 33 CEGs for *S. suis* P1/7 grown in APS and 25 CEGs in CSF, both compared to growth in THY control medium (Table 1).

Genes identified by Tn-seq exhibiting fitness impact in S. suis growth in APS compared to THY

The transposon library was cultivated for approximately 4 hours in THY or APS and Tn-seq was used to identify CEGs that support the growth of *S. suis* in APS. Out of the 33 CEGs (Table 1), 7 (21%) did not have annotations in NCBI nor KEGG database. Among the annotated genes, 10 (30%) were predicted to be involved in metabolism, 5 (15%) in nucleotide metabolism and 8 genes (24%) in substrate transport. Thus "metabolism" and "substrate transport" were the most abundant annotations of CEGs linked to the growth of *S. suis* in APS (Figure 2). Furthermore, 3 genes were annotated as transcription factors, 2 as oxidoreductases, 1 as a signal transduction protein, and 1 as methyltransferase.

Of the 10 genes annotated as substrate transporters, 3 genes were predicted to belong to a tryptophan ABC transporter, 3 genes to an amino acid ABC transporter, and 1 gene (gene symbol *ptsP*) as a component of a sugar transporter. The remaining 3 genes were part of a single operon with unknown function. In this operon, a predicted substrate-binding lipoprotein (SSU_RS04755) is highly conserved across *S. suis* strains, including strains from serotype 2 and 9 [41]. This protein is also part of the *S. suis* secretome, and has been studied as a potential vaccine candidate targeting *S. suis* [41,42]. An amino acid sequence homology search using NCBI blastp tool revealed a high identity (> 60%) with ABC transporters described as nucleoside transporters from *S. pneumoniae* (SPD_0739) and *Streptococcus agalactiae* (GBS0942) [43,44]

Genes identified by Tn-seq contributing to S. suis growth in CSF compared to THY

To explore whether nucleotide metabolism and transport pathways also play a critical role in *S. suis* growth in CSF, we performed a Tn-seq screen comparing growth in CSF and THY. In contrast to APS, no genes involved in nucleotide metabolism or transport were conditionally essential for *S. suis* growth in CSF. *S. suis* CEGs supporting growth in CSF included 8 genes (32%) annotated with roles in amino acid transport, 7 genes (28%) annotated as hypothetical proteins, 3 genes annotated with roles in carbohydrate metabolism, and 2 genes annotated as transcriptional regulators (Table 1, Figure 2).

We found 8 CEGs that supported growth in both CSF and APS. The three genes that are predicted to form a tryptophan ABC transporter were identified as conditionally essential in both media (Table 2). Additionally, SSU_RS07195, annotated as a hypothetical protein, and SSU_RS02715, annotated as a cystine-binding lipoprotein, were also identified as conditionally essential for growth in CSF and APS. Transposon insertions in *liaF*, a membrane protein, and the hypothetical protein SSU_RS07195, were associated with increased proliferation during growth in CSF compared to THY, whereas insertions in the same genes (*liaF* and SSU_RS07195), were associated with reduced proliferation in APS compared to THY. Lastly, transposon insertions in the phosphate importer *pstB3_1* were associated with increased proliferation in APS but reduced proliferation in CSF.

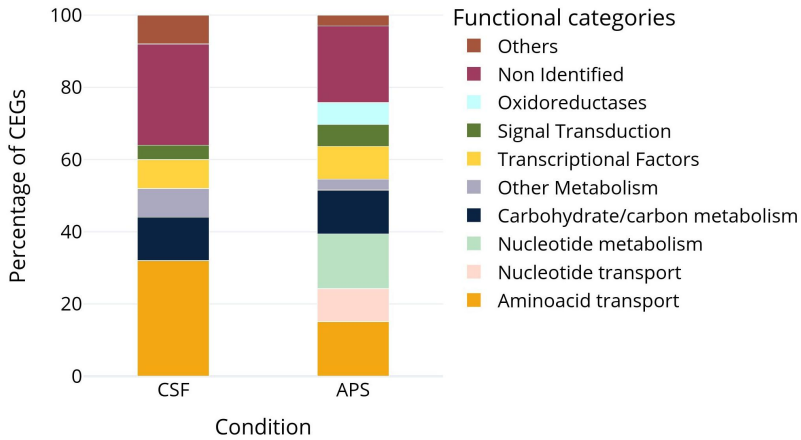

Figure 2. Stacked bar chart showing the percentage of CEGs (log_2FC < −1, adjusted p-value < 0.05) classified into functional categories for CSF and APS samples.

Table 2. Shared genes identified by Tn-seq analysis of *S. suis* P1/7 in APS and CSF media (adj. p-vale <0.05; $Log_2FC < -1$; $Log_2FC > 1$). Genes belonging to the same operon are marked with the same symbol in the "Operons" column. Genes with decreased fitness (negative Log_2FC) are highlighted in orange, and genes with increased fitness (positive Log_2FC) are highlighted in green.

Common genes identified by Tn-seq in APS and CSF					
Locus tag	**Name**	**Product**	**Operons**	**Log_2FC APS**	**Log_2FC CSF**
SSU_RS06600	-	ABC transporter permease	□	**-2.28**	**-2.88**
SSU_RS06605	*trpX*	tryptophan ABC transporter substrate-binding protein	□	**-1.84**	**-2.97**
SSU_RS06595	-	ABC transporter ATP-binding protein	□	**-1.73**	**-2.63**
SSU_RS07155	-	Hypothetical protein		**-1.34**	**-1.43**
SSU_RS02715	fliY	L-cystine-binding protein FliY		**-1.26**	**-1.14**
SSU_RS07195	-	Hypothetical protein		**-1.18**	**1.56**
SSU_RS02080	*liaF*	cell wall-active antibiotics response protein LiaF		**-1.21**	**1.3**
SSU_RS04835	pstB3_1	Phosphate import ATP-binding protein PstB 3		**2.17**	**-2.13**

Validating Tn-seq results using in frame deletion mutants

To validate the Tn-seq results, we selected 5 CEGs identified in APS (*purA*, SSU_RS04755, *liaF*, SSU_RS09155 and SSU_RS07155; Table 1) to make in-frame deletions in *S. suis* strain P1/7. Given that genes related to nucleotide metabolism and transport were the most represented among the CEGs (Figure 2), we hypothesized that nucleotide availability was a limiting factor for *S. suis* growth in serum. We chose to generate a *purA* (SSU_RS08850) deletion mutant strain because (i) *purA* was annotated as playing a role in nucleotide metabolism; (ii) showed the highest log_2FC difference (−3.19) in the list of CEGs, and (iii) was reported as a CEG for *S. suis* survival in pigs in previous Tn-seq studies [30]. SSU_RS04755 was selected because it is within a predicted nucleoside ABC transporter operon. Additionally, we selected the predicted *liaF* (SSU_RS02080) gene, annotated as participating in signal transduction. We had found that *liaF* was conditionally essential when *S. suis* was cultured in APS, with a negative log_2FC, and its inactivation increased fitness in CSF resulting in positive log_2FC (see above). This suggests a differential role for *liaF* in growth under these two culture conditions. In various Gram-positive bacteria, *liaF* is part of a three-component system, along with a histidine kinase (*liaS*) and a transcription regulator (*liaR*) [45]. *LiaFSR* is involved in virulence and antibiotic resistance in streptococci [46,47], but it has not been studied in *S. suis*. We were unable to obtain a viable *liaF* deletion mutant. Downstream of *liaF* are *liaS* (SSU_RS02085) and *liaR* (SSU_RS02090), which have overlapping reading frames and are controlled by the same promoter. Thus, we hypothesized that transposon insertions in *liaF* would disrupt the transcription of *liaS* and *liaR* and generated gene deletion mutants for *liaS* and *liaR* as a proxy for *liaF* gene deletion.

From the group of unknown genes of APS CEGs list, we selected SSU_RS09155, which had the highest fold change (Table 1) and SSU_RS07155, which is predicted to encode a protein with unknown function and demonstrated a negative fold change in both APS and CSF. From the CEGs list in CSF, we also selected SSU_RS02635, encoding a protein with unknown function, and a log_2FC change of −3,22 in CSF.

Site-specific gene deletion mutants were generated using our previously described CRISPR-Cas gene deletion method (Gussak et al.; see Methods) and verified by PCR amplification of the corresponding locus. Growth rates in THY and APS were assessed by OD_{600} measurements and CFU counting each hour during an 8-hr period (Figure 3). In THY medium, the mutant strains had the same growth rate as the WT across all phases of the growth curve, except for the *liaR* mutant, which had a one-log_{10} reduced CFU count in the stationary phase (Figure 3). In APS, the Δ*purA* mutant exhibited growth attenuation compared to the WT, reaching a maximum concentration of approximately 10^7 CFUs/mL, whereas the WT

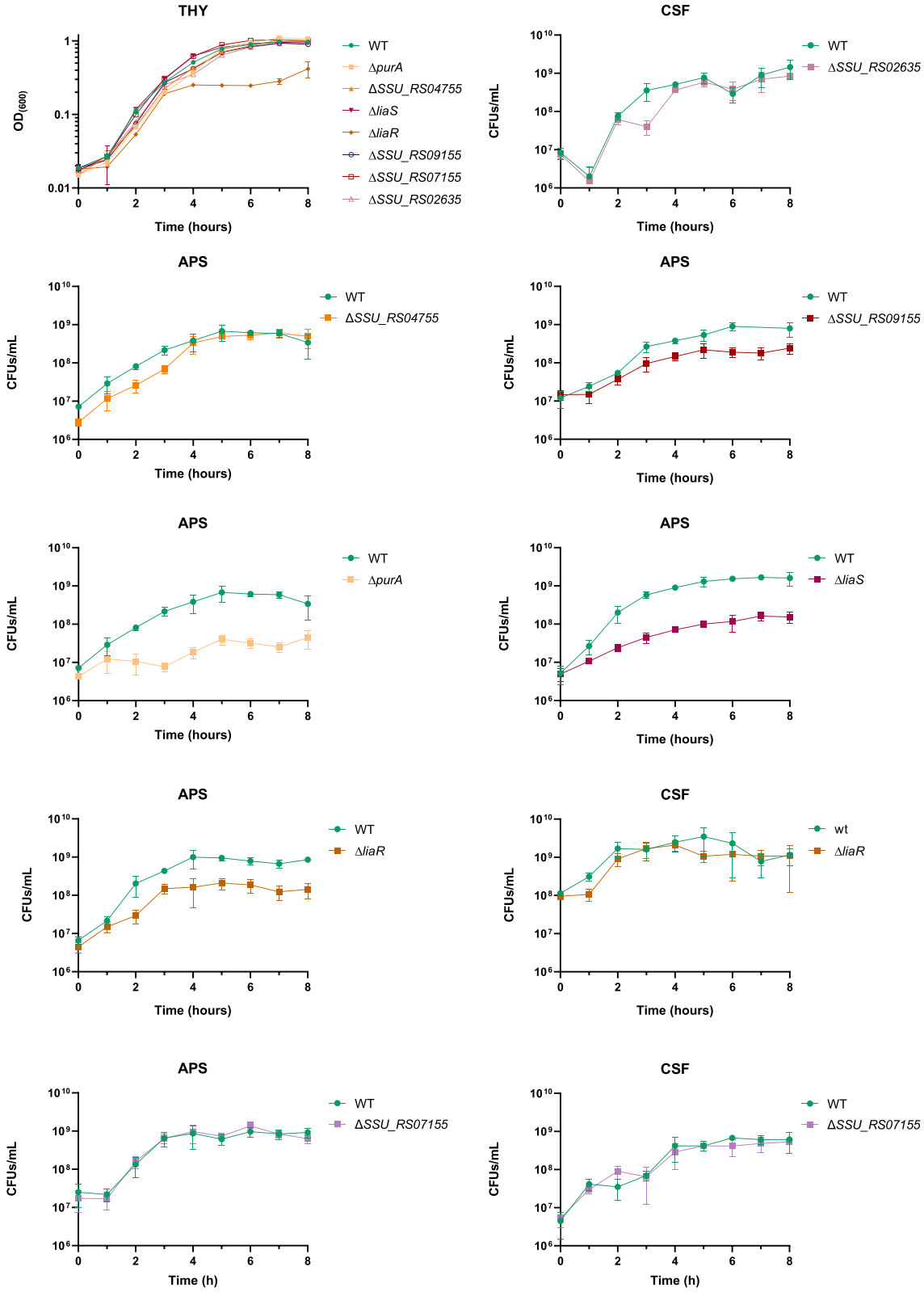

Figure 3. Growth curves in thy, APS and CSF. Data shown are means ± standard deviation of at least two biological replicates and two technical replicates for CFUs counting. CFUs/mL and OD_{600} axis are in Log_{10}.

reached a concentration of nearly 10^9 CFUs/mL. This growth defect correlated with the Tn-seq data, where *purA* had a log_2FC difference of −3.19, indicating that functional PurA contributes to the growth of *S. suis* P1/7 in APS. Growth assays in APS showed that Δ*liaR*, Δ*liaS* and ΔSSU_RS09155 gene deletion-mutants

exhibited a growth delay during the exponential phase and reached stationary phase with lower bacterial cell densities compared to the WT, confirming the APS Tn-seq results (Figure 3). The *liaR* mutant did not exhibit any difference in growth in CSF compared to the WT parental strain, whereas in CSF, the Tn-seq results revealed a positive $\log_2$FC for *liaR*. The ΔSSU_RS04755 mutant exhibited a delayed growth rate compared to the WT during the first 3 hr of growth in APS, although the mutant ultimately reached the same bacterial densities at stationary phase as WT. Mutants ΔSSU_RS07155 and ΔSSU_RS02635 did not show significantly altered growth curves in any of the tested conditions.

LiaR activates transcription of the hypothetical protein SSU_RS07195

Deletion of the gene encoding transcriptional regulator LiaR led to lower growth in APS. We hypothesized that LiaR may regulate a gene(s) critical for growth in APS. If our hypothesis were correct, we expected that some of the genes regulated by LiaR might feature in our Tn-seq results. To explore this, we used FIMO (Find Individual Motif Occurrences, part of the MEME online software suite, see Methods) to search for potential LiaR binding sites across the *S. suis* genome (Table S3). FIMO predicted presence of a putative LiaR binding site in the promoter of one of the genes encoding a hypothetical protein, SSU_RS07195, one of the genes identified as CEGs in the APS Tn-seq results. To investigate possible functions of the hypothetical protein encoded by SSU_RS07195, we examined genomic position and neighborhood of SSU_RS07195 in *S. suis* P1/7 in the NCBI database, and found the gene to be partially overlapping with gene SSU_RS07190, possibly part of a single operon together with a third gene SSU_RS10200 encoding an IS630 family transposase (Figure 4). The second gene SSU_RS07190 was predicted to encode a hypothetical protein containing a phage-shock protein (PspC) domain (Figure 4(a)).

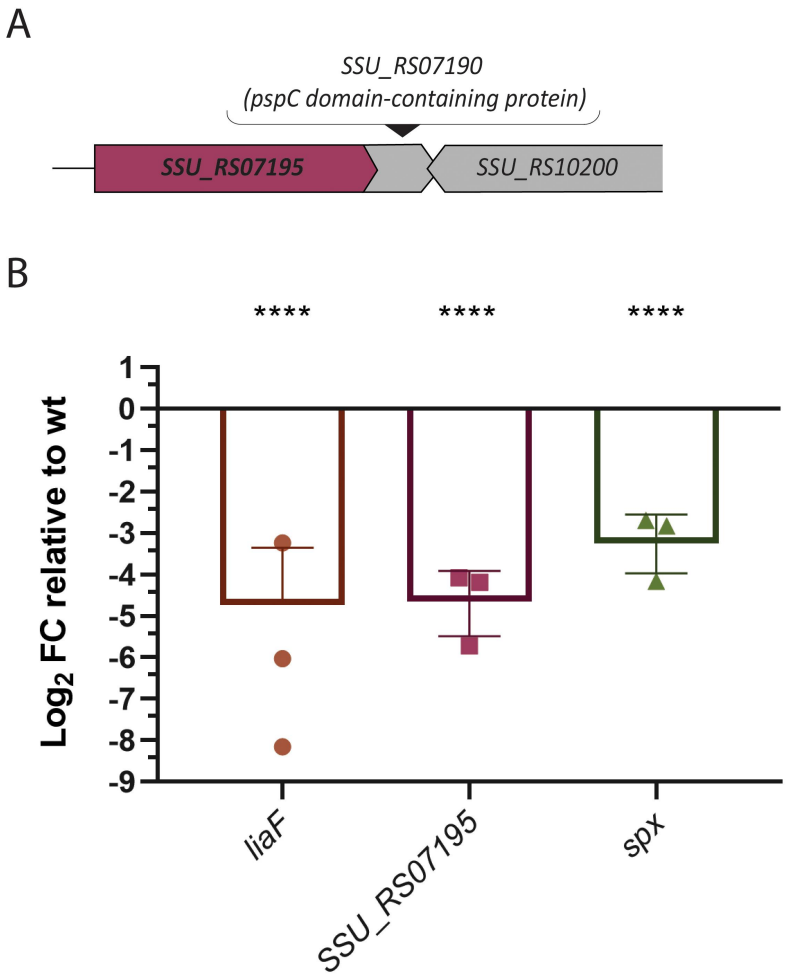

Figure 4. (A) schematic representation of the SSU_RS07195 operon. (B) expression of *liaF*, SSU_RS07195, and *spx* in the LiaR mutant relative to WT. Error bars represent standard deviation across biological replicates. Statistical analysis was performed using a one-way ANOVA followed by Dunnett's multiple comparisons test (****$p < 0.0001$).

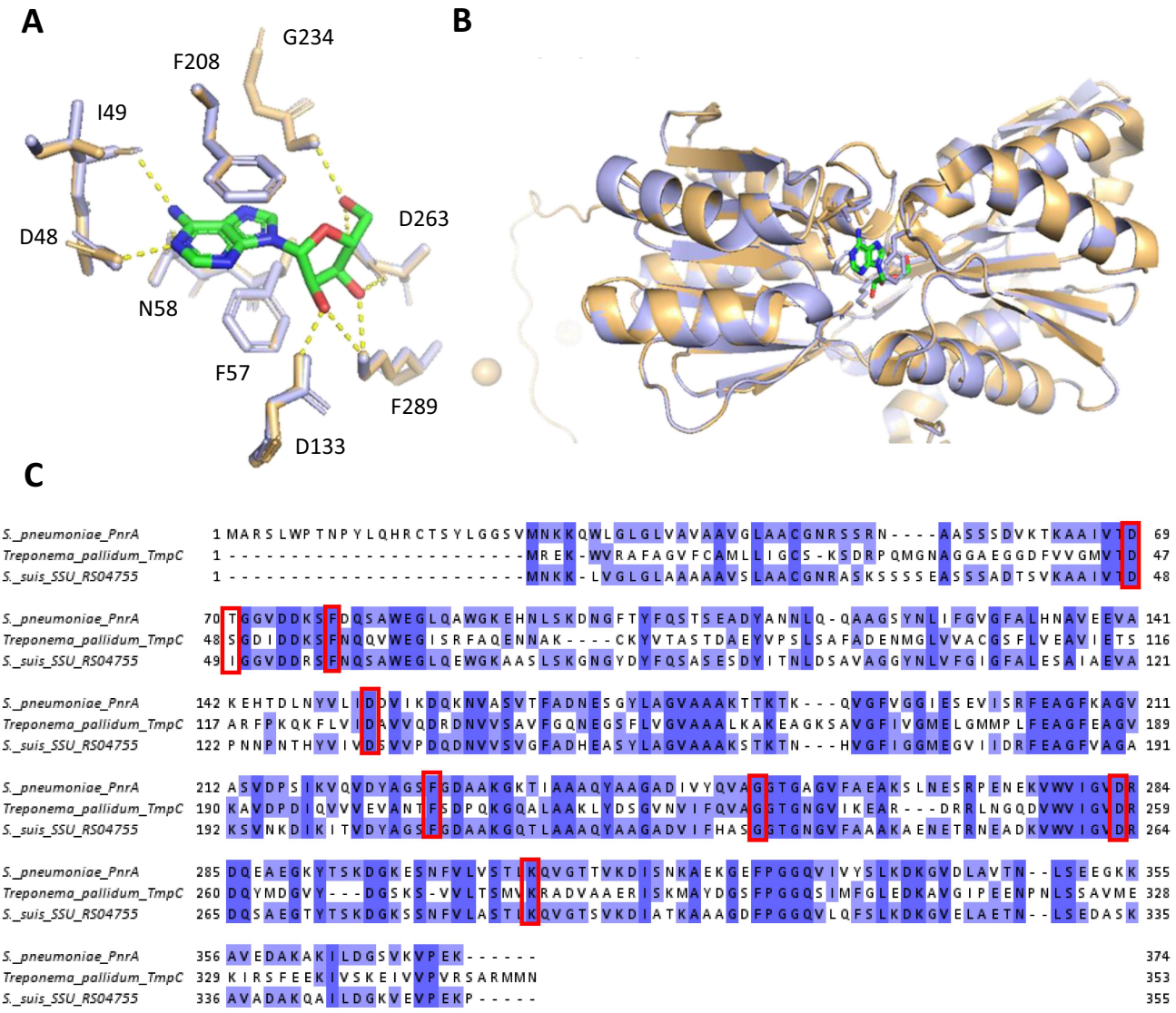

Figure 5. Structural and sequence analysis of protein homologs featuring *S. suis* lipoprotein SSU_RS04755 (blue) and *S. pneumoniae* PnrA (PDB id: 6Y9U, orange). (A) zoomed-in view of the binding pocket with hydrogen bond interactions (dashed yellow lines). (B) Ribbon representation of the structural alignment of both proteins, highlighting active site interactions with a ligand (green) and key residues (sticks). (C) Multiple sequence alignment of homologous proteins from *S. pneumoniae*, *T. pallidum*, and *S. suis*, with conserved residues highlighted in blue and functionally significant residues marked with red boxes.

Both genes appear to be controlled by the same promoter, as the downstream gene lacks an independent promoter region, and the 5' end of SSU_RS07190 overlaps with the end of SSU_RS07195. Both *liaF* and SSU_RS07195 are CEGs supporting the growth of *S. suis* P1/7 in APS with a negative $\log_2$FC (−1.21 and −1.18, respectively; Table 1). To validate these predictions, we performed qPCR to determine whether the expression of SSU_RS07195 was altered in the Δ*liaR* gene deletion mutant using *liaF* and *spx* genes, known to be regulated by LiaR in other species [45,48], respectively, as references for comparison. Indeed, qPCR results showed that the expression of SSU_RS07195 was significantly reduced in *liaR* gene deletion mutant compared to WT, suggesting that LiaR, directly or indirectly, positively regulates expression of SSU_RS07195 (Figure 4). *liaF* and *spx* also showed reduced expression in *liaR* gene deletion mutant. Notably, the amount of downregulation of SSU_RS07195, −4.5 $\log_2$FC (Figure 4), was similar in magnitude to that observed for *liaF* and *spx*, −4.6, and −3.09 $\log_2$FC, respectively (Figure 4).

In silico *analysis of* S. suis *SSU_RS04755*

Gene SSU_RS04755 has been predicted to encode a basic membrane family protein (BMP), a transmembrane component of specific ABC

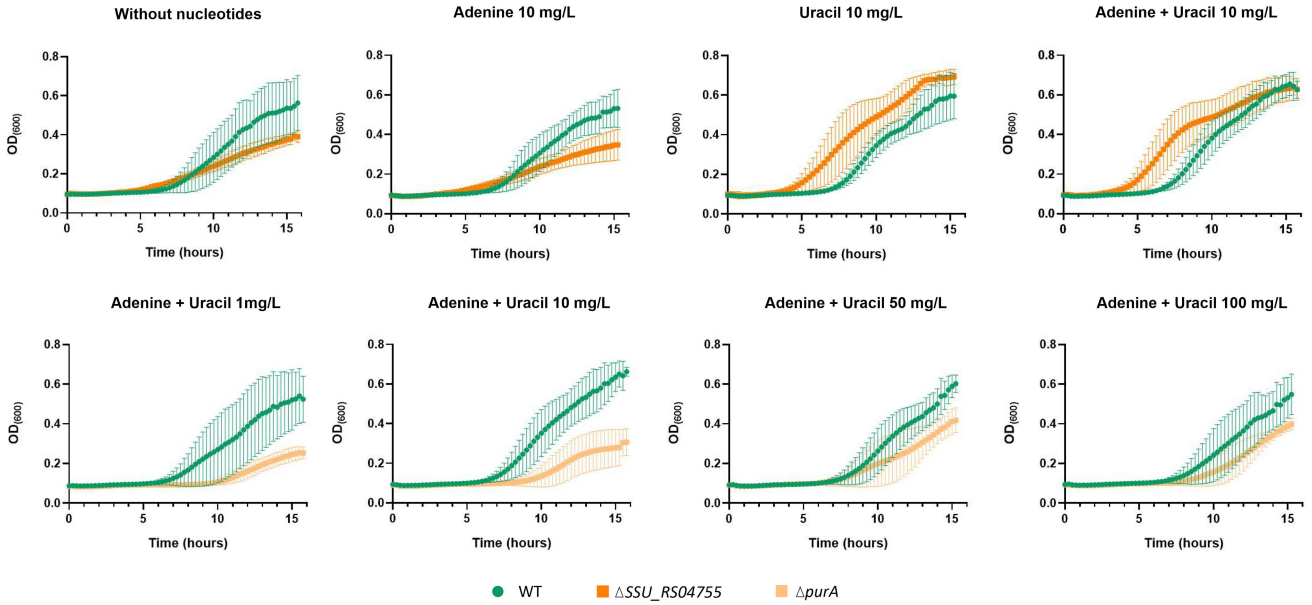

Figure 6. Growth curves of WT (green), *purA* (light orange) and ΔSSU_RS04755 (dark orange) in CDM. (a) WT and ΔSSU_RS04755 growth with different availability of adenine and uracil. (b) WT and Δ*purA* growth with increasing concentrations of adenine and uracil. The experiments were performed with at least 3 biological replicates of each strain. Data shown are means ± standard deviation.

transporters. Growth curve experiments did not reveal a significant reduction in the growth rate of our ΔSSU_RS04755 mutant. The operon genes with SSU_RS04755 were predicted to encode an ATP-binding protein and a permease which are typical components of an ABC transporter. Both predicted ATP-binding protein and permease encoding genes appeared as CEGs in our Tn-seq results (Table 1). The protein sequence associated with SSU_RS04755 shares significant identity with lipoproteins that are components of nucleoside ABC transporters in Gram-positive bacteria (see above), suggesting that SSU_RS04755 and its operon genes may encode an ABC transporter complex involved in nucleoside transport. To investigate the possible functional equivalence of SSU_RS04755 operon genes with ABC transporters, we performed amino acid sequence alignments of SSU_RS04755 with PnrA and TmpC, which are homologous nucleoside binding lipoproteins from *S. pneumoniae* and *Treponema pallidum (T. pallidum)* respectively [49,50]. Using the crystal structure of PnrA binding to adenosine [49], we confirmed that all but one (T70) of the specific amino acids involved in adenosine binding by PnrA were conserved in SSU_RS04755 (Figure 5(c)). To verify if the structural positions of these amino acids were conserved, we performed a structural prediction (see methods) of the predicted *S. suis* lipoprotein SSU_RS04755 and aligned it to the structure of PnrA (ID 6y9U in Protein Data Bank (PDB). We confirmed that all amino acids involved in the adenosine binding are located at the same position in both protein structures. The non-conserved amino acid T70 which is I49 in *S. suis* might bind adenosine, as it has a carboxyl group (COOH) in the same position as the corresponding residue in PnrA that is involved in adenosine binding (Figure 5(a,b)).

*Growth in CDM reveals nucleobase uptake deficiencies of ΔSSU_RS04755 and growth reduction of Δ*purA *mutant*

To further investigate our hypothesis that SSU_RS04755, SSU_RS04750, and SSU_RS04745 are part of an ABC transporter for nucleosides, we grew the ΔSSU_RS04755 mutant in CDM containing varying concentrations of purines and pyrimidines. When adenine was added to the CDM (Figure (6a)), the ΔSSU_RS04755 mutant showed reduced growth compared to the WT, reaching an OD_{600} of approximately 0.4 versus 0.6 for the WT. Interestingly, the growth of both WT and ΔSSU_RS04755 with adenine supplementation was similar to their growth without nucleobases, suggesting a defect in the ΔSSU_RS04755 mutant's ability to uptake adenine. We observed that WT grew the same with and without addition of nucleobases, which might suggest that during preculture in THY

prior to CDM growth assays, WT bacteria stored nucleobases intracellularly. However, following the same preculturing step in THY, the growth of the corresponding ΔSSU_RS04755 deletion mutant in CDM, with adenine as sole source of nucleobase, was substantially lower, in agreement with the hypothesis that SSU_RS04755 encodes a protein that is part of an ABC transporter importing nucleobases.

A second CEG, *purA*, was annotated to encode an adenylosuccinate synthase enzyme that is involved in the conversion of IMP (inosine monophosphate) to AMP (adenosine monophosphate). We hypothesized that the growth deficiency of the *purA* mutant in APS might have been due to its inability to synthesize adenine. We assessed the growth of the *purA* mutant in CDM with increasing concentrations of nucleobases to compensate for the lack of *de novo* synthesized purines in the deletion mutant. Surprisingly, the addition of nucleobases could not recover the WT phenotype: the Δ*purA* deletion mutant exhibited a pronounced decrease in growth rate compared to the WT, reaching a maximum OD_{600} of approximately 0.4, whereas the WT OD_{600} reached up to 0.7. This phenotype was consistent regardless of the concentration of nucleobases added to the CDM (Figure (6b)).

Discussion

In this study, we constructed a transposon mutant library (Tn-library) for *S. suis* strain P1/7 and employed transposon sequencing (Tn-seq) to screen for CEGs that mediated growth of *S. suis* bacteria in two host body fluids, activated porcine serum (APS) and cerebrospinal fluid (CSF). APS was selected to simulate bloodstream conditions, as it supports more reproducible *S. suis* growth than whole blood, which likely restricts growth through neutrophil activation and antimicrobial peptide release [51]. Additionally, we chose to perform Tn-seq in CSF since virulent *S. suis* strains like P1/7 are able to grow in CSF. Using APS and CSF allowed controlled library screening while minimizing stochastic selection of mutants typical of *in vivo* models [52]. The library quality was high, with saturation of potential TA-insertion sites ranging from 44% to 67% and an average coverage of 91% across coding regions, well above the ≥35% TA-site coverage threshold reported to yield reliable essentiality predictions in *Streptococcus* [53]. To our knowledge, this is the first study to apply an in-house Nanopore sequencing approach to Tn-seq in *S. suis*. For downstream analysis, we designed a Tn-Seq data analysis pipeline to analyze nanopore sequencing output and generate a list of CEGs, which is publicly available to support community reuse. Running ONT in-house improved access and speed, enabling rapid turnaround and iterative screening without reliance on external services. ONT data supported accurate insertion mapping, as reflected by consistent insertion-site assignments across conditions and replicated growth phenotypes in independently reconstructed mutants.

The Tn-seq results revealed a list of 33 and 25 CEGs that appeared crucial for optimal *S. suis* growth in APS and CSF, respectively. According to the functional annotations of the crucial genes mediating growth in APS, the main biological processes regulated by these genes were *de novo* biosynthesis of nucleotides and ABC transport systems. Genes conditionally essential for growth in CSF were primarily involved in amino acid transport. Five genes were common to both lists; three of these were part of a tryptophan ABC transporter operon, which has been previously reported as conditionally essential in Tn-seq studies on *S. suis*, corroborating reports that *S. suis* can not synthesize tryptophan [30,54]. In APS, a substantial number of genes were annotated to be involved in nucleotide metabolism and nucleotide transport. Arenas and colleagues and Dresen and colleagues studied genes supporting *S. suis* growth in blood and CSF using a porcine *in vivo* Tn-library approach, and found that genes involved in *de novo* nucleotide biosynthesis, such as *purA, purB*, and *guaA*, were conditionally essential in both fluids [30,54]. The genes *purA* and *guaB* were also reported as CEGs for growth of Group A *Streptococcus* (GAS) in human blood [55], suggesting that genes related to nucleotide metabolism and transport are important for survival of streptococci in APS. Our Tn-seq screening in CSF did not identify CEGs annotated with functions in nucleotide biosynthesis. However, it revealed an enrichment of 10 genes involved in protein synthesis, 8 of which were annotated with functions in amino acid transport systems. This finding is consistent with reports showing that CSF contains lower amino acid levels than serum [27], which may necessitate the upregulation of amino acid transport systems for growth. Notably, these same studies identified inosine, a purine nucleoside that plays an essential role in purine nucleotide biosynthesis, as one of the metabolites found exclusively in CSF [27]. This may explain the absence of CEGs annotated with functions in nucleotide transport and biosynthesis pathways in the Tn-seq results from CSF, as inosine in CSF could act as a readily available precursor for purine nucleotide synthesis.

From our list of CEGs in APS, five genes, i.e. *purA*, SSU_RS04755, *liaF*, SSU_RS09155, and SSU_RS07155

were selected for verification of the library results by generating gene-specific in-frame deletion mutants. From our list of CEGs in CSF, genes SSU_RS02635, and SSU_RS07155 with negative FC and *liaR* with positive FC were selected for verification. The choice of these genes was based on: (i) enrichment of certain biological processes according to CEGs annotations; (ii) genes identified in Tn-library based studies in different streptococci, i.e. *purA* and *liaF*; (iii) uncharacterized genes in *S. suis* of possible interest, e.g. located in an operon with a gene of interest; and (iv) the presence of a CEG in APS and CSF. We failed in obtaining viable *liaF* deletion mutants, but could obtain deletion mutants of operon genes *liaS* and *liaR*. Deletion mutants of the genes *purA, liaR, liaS* and SSU_RS09155 had lower growth rates in APS and reached lower CFU/mL counts in the stationary phase compared to the WT strain, thus validating the Tn-seq results. The *liaR* deletion mutant showed no growth deficiency in CSF compared to the WT, thus confirming the results obtained for this gene in CSF. Gene deletion mutants for the genes SSU_RS04755, SSU_RS02635, and SSU_RS07155 did not exhibit any significant reduction in growth rate under any of the conditions tested. This could be due to differences between pooled Tn-Seq selection, where mutants compete within a mixed library, and single-strain validation in a pure culture. Additionally, polar effects of transposon insertions on downstream genes may contribute to signals not reproduced by targeted knockouts.

In silico analysis suggested that gene SSU_RS04755 encodes a lipoprotein that is part of a nucleotide ABC transporter. Notably, all three genes in the SSU_RS04745–55 operon were identified as CEGs in APS, underscoring the importance of this nucleotide ABC transporter for survival in serum-like conditions, highlighting the importance of this candidate nucleotide ABC transporter to support *S. suis* growth in APS. Our growth experiments in CDM demonstrated that the SSU_RS04755 gene deletion mutant showed significant growth reduction when purines were the sole source of nucleobases, suggesting its essential role in purine uptake. Taken together, these results support the *in silico* predictions that the SSU_RS04745-55 operon encodes an ABC transporter for purine uptake. In *S. pneumoniae* a nucleoside transporter with 66% homology to the *S. suis* SSU_RS04745-55 candidate purine transporter was shown to be important for growth in serum. Additionally, *S. pneumoniae* Δspd_0739 mutant, lacking a lipoprotein that is part of a nucleotide transport system, exhibited reduced virulence compared to WT [56] The spd_0739 lipoprotein component of the transporter was proposed as a vaccine candidate due to its high conservation among strains (> 98%), its expression both *in vitro* and during *in vivo* infection, and its low homology (< 11%) with human lipoproteins [56]. In *Borrelia burgdorferi*, two purine uptake transporters are important for *in vivo* infection, while mutants grow normally in rich media [57], paralleling our observation that ΔSSU_RS04755 is impaired only under purine limitation.

We identified the genes *purA, purB*, *guaA, guaB,* and *pyrE* involved in *de novo* nucleotide biosynthesis as CEGs supporting *S. suis* growth in APS. Previous studies had shown that disruption in the purine biosynthesis pathways may reduce bacterial colonization and intracellular growth, increase susceptibility to oxidative stress, and lower bacterial proliferation in human serum and blood [58–61]. Additionally, genome-wide screens in *Staphylococcus aureus (S. aureus)* demonstrated that *pur* and *pyr* gene deletion mutants were attenuated in various infection models [62–65]. The importance of the nucleotide biosynthesis pathway is not surprising, as it is (i) essential for the synthesis of nucleic acids; (ii) mediating the production of signaling molecules like cyclic AMP and GMP and (iii) generating energy storage molecules such as ATP and GTP [66]. Our *S. suis* P1/7 *purA* mutant showed significant growth defects in CDM and was not rescued by the addition of nucleobases, suggesting that in limited-nutrient media, nucleobases uptake could not rescue viability-lowering effects of *purA* deletion. It thus appears that nucleobase uptake and salvage pathways alone are insufficient to meet the purine demands of the *S. suis* P1/7 Δ*purA* mutant. However, while several studies in other bacterial genera such as *Escherichia*, *Salmonella*, and *Bacillus* have demonstrated successful growth restoration of *pur* and *pyr* mutants following the addition of nucleobases to the media [60,67], no studies have been found regarding growth restoration in *Streptococcus*. Given that *de novo* purine biosynthesis involves an extensive list of *pur* genes, it appears that mutations at different points in the pathway may produce distinct phenotypic effects such that compensatory mutations or pathway rerouting is usually not restoring viability or growth recovery. In studies where growth recovery had turned out possible, deleted genes were typically at the beginning of the pathway, such as *purF* and *purE* [60,67]. In contrast, in *S. suis* P1/7, *purA* is located toward the end of the pathway (KEGG. *Purine metabolism – Pathway ID: ssi00230)* and may therefore result in more pronounced phenotypic changes. The significance of *purA* in pathobiology is further highlighted by a study in clinical *S. aureus*, where it was found that *purA* was induced

when *S. aureus* entered into a semi-dormant state in the human body upon exposure to acidic pH or neutrophils as part of the immune response to *S. aureus* infection [68].

Our study revealed the important regulatory role of the LiaFSR three-component system in mediating *S. suis* growth in APS, with a particular focus on the regulatory function of LiaR. Our data suggest that LiaR is acting directly or indirectly, as a positive regulator of at least one CEG involved in supporting *S. suis* growth in APS, highlighting its role in stress adaptation and environmental sensing. Future work using direct DNA-binding assays will be needed to confirm whether LiaR targets the promoters of these genes. Of note, *liaF* and gene SSU_RS07195 encoding a hypothetical protein displayed negative $\log_2$FC values during growth in APS, but positive $\log_2$FC values during growth in CSF, implying that LiaFSR activation is advantageous in APS, while its repression may be beneficial or neutral in CSF. This key role of the LiaFSR sensory system in adapting to different host niches and nutrient availability has been described previously by Sanson and colleagues [48] who reported that in *Streptococcus pyogenes*, a mutant not producing LiaR showed reduced expression of virulence genes including *spxA2*, which is involved in oxidative stress response, in an *ex vivo* human blood model. We found that our *S. suis* P1/7 *liaR* gene deletion mutant exhibited reduced growth during culture in APS, a model for growth in blood (*S. suis* P1/7 cannot be cultured reproducibly in whole blood) while the deletion of *S. suis* P1/7 *liaR* did not reduce bacterial growth during culture in CSF; instead, our Tn-seq data suggested that deletion of *liaR* was associated with increased bacterial growth in CSF. These results highlight the metabolic flexibility that disease-associated bacteria can be capable of in order to rapidly alter gene expression to adapt to different host niches. These results also reinforce the notion that some candidate antibacterial targets are only expressed in specific host niches, so that treatments including vaccinations should take such niche-specific antibacterial target expression into account when treating bacterial infections. Given the limited robustness of current *S. suis* infection models and the invasiveness of CSF access, porcine challenge studies are best reserved for well prioritized candidates with clear translational potential. Future work will evaluate selected high confidence CEGs in focused porcine infection studies [16,69].

Acknowledgements

We thank Tim Van Opijnen's lab (Tufts University) for the transposon library protocol and plasmids, and Alex Gussak (Wageningen University & Research) for the CRISPR-Cas9 protocol for *S. suis* mutants design.

Author contributions

CRediT: **Maria Juanpere-Borras:** Conceptualization, Formal analysis, Investigation, Methodology, Supervision, Validation, Visualization, Writing – original draft, Writing – review & editing; **Tiantong Zhao:** Investigation, Methodology; **Jos Boekhorst:** Data curation, Formal analysis, Methodology, Software; **Blanca Fernandez-Ciruelos:** Conceptualization, Methodology, Supervision; **Rajrita Sanyal:** Investigation; **Nissa Arifa:** Investigation; **Troy Wagenaar:** Investigation; **Peter van Baarlen:** Conceptualization, Funding acquisition, Supervision, Writing – review & editing; **Jerry M. Wells:** Conceptualization, Funding acquisition, Resources, Supervision, Writing – review & editing.

Funding

This research has received funding from the European Union's Horizon 2020 research and innovation program under the Marie Sklodowska-Curie grant agreement number 956154. Tiantong Zhao received additional funding from the China Scholarship Council (No. 201906350084). Nissa Arifa was supported by the Research Center for Genetic Engineering, National Research and Innovation Agency (BRIN), Bogor, Indonesia.

Disclosure statement

No potential conflict of interest was reported by the author(s).

Data availability statement

All sequencing data generated in this study (FAST5 and FASTQ files) are openly available in the European Nucleotide Archive (ENA) at https://www.ebi.ac.uk/ena/browser/view/PRJEB89170 [70]. The raw result files generated by the Tn-Seq analysis, and data supporting all figures in the manuscript are openly available in the 4TU.ResearchData repository at https://data.4tu.nl/datasets/ace99cb5-0414-4a91-9aa8-72c0d8c47381/1 [71]. All data are available under a Creative Commons CC-BY 4.0.

Use of generative AI

During the preparation of this manuscript, the authors utilized ChatGPT (OpenAI, GPT-4 May 2024 version) to enhance the clarity of the text and assist in developing code for figure generation. All AI-assisted content was reviewed and edited by the authors to ensure accuracy and integrity.

ORCID

Maria Juanpere-Borras http://orcid.org/0000-0003-0581-0937
Jos Boekhorst http://orcid.org/0000-0002-4807-7838
Blanca Fernandez-Ciruelos http://orcid.org/0000-0002-7532-2704
Peter van Baarlen http://orcid.org/0000-0003-3530-5472

References

[1] Zhao T, Pellegrini L, van der Hee B, et al. Choroid plexus organoids reveal mechanisms of *Streptococcus suis* translocation at the blood-cerebrospinal fluid barrier. Fluids Barriers CNS. 2025;22(1):14. doi: 10.1186/s12987-025-00627-y

[2] Feng Y, Zhang H, Wu Z, et al. *Streptococcus suis* infection: an emerging/reemerging challenge of bacterial infectious diseases? Virulence. 2014;5(4):477–497. doi: 10.4161/viru.28595

[3] Weinert LA, Chaudhuri RR, Wang J, et al. Genomic signatures of human and animal disease in the zoonotic pathogen *Streptococcus suis*. Nat Commun. 2015;6(1):6. doi: 10.1038/ncomms8272

[4] Arenas Busto J. Streptococcus suis: Methods and Protocols. New York (NY): Humana Press; 2024. Available from: http://www.springer.com/series/7651. doi: 10.1007/978-1-0716-3898-9

[5] Ho DTN, Le TPT, Wolbers M, et al. Risk factors of *Streptococcus suis* infection in Vietnam. A case-control study. PLOS ONE. 2011;6(3). doi: 10.1371/journal.pone.0017604

[6] Segura M. *Streptococcus suis* research: progress and challenges. Pathogens. 2020;9(9):1–8. doi: 10.3390/pathogens9090707

[7] Takeuchi D, Kerdsin A, Akeda Y, et al. Impact of a food safety campaign on *Streptococcus suis* infection in humans in Thailand. Am J Trop Med Hyg. 2017;96(6):1370–1377. doi: 10.4269/ajtmh.16-0456

[8] Mai NTH, Hoa NT, Nga TVT, et al. *Streptococcus suis* meningitis in adults in Vietnam. Clin Infect Dis. 2008;46(5):659–667. doi: 10.1086/527385

[9] Wertheim HFL, Nghia HDT, Taylor W, et al. *Streptococcus suis*: an emerging human pathogen. Clin Infect Dis. 2009;48(5):617–625. doi: 10.1086/596763

[10] Segura M, Calzas C, Grenier D, et al. Initial steps of the pathogenesis of the infection caused by *Streptococcus suis*: fighting against nonspecific defenses. FEBS Lett. 2016;590(21):3772–3799. doi: 10.1002/1873-3468.12364

[11] Staats JJ, Feder I, Okwumabua O, et al. *Streptococcus suis*: past and present. Vet Res Commun. 1997;21(6):381–407. doi: 10.1023/A:1005870317757

[12] Isabela Maria Fernandes de Oliveira. Exploiting the tonsil microbiota to prevent *Streptococcus suis* infections. Wageningen, The Netherlands: Wageningen University; 2023.

[13] Segura M, Gottschalk M. *Streptococcus suis* interactions with the murine macrophage cell line J774: adhesion and cytotoxicity. Infect Immun. 2002;70(8):4312–4322. doi: 10.1128/IAI.70.8.4312-4322.2002

[14] Williams A, Blakemore W. Pathogenesis of meningitis caused by *Streptococcus suis* type 2. J Infect Dis. 1990;162(2):474–481. doi: 10.1093/infdis/162.2.474

[15] Tram G, Jennings M, Blackall P, et al. *Streptococcus suis* pathogenesis—a diverse array of virulence factors for a zoonotic lifestyle. Adv Microb Physiol. 2021;78:217–257. doi: 10.1016/bs.ampbs.2020.12.002

[16] Segura M, Fittipaldi N, Calzas C, et al. Critical *Streptococcus suis* virulence factors: are they all really critical? Trends Microbiol. 2017;25(7):585–599. doi: 10.1016/j.tim.2017.02.005

[17] Murray G, Hossain A, Miller E, et al. The emergence and diversification of a zoonotic pathogen from within the microbiota of intensively farmed pigs. Proc Natl Acad Sci USA. 2023;120(47). doi: 10.1073/pnas.2307773120

[18] Roodsant TJ, Van Der Putten BCL, Tamminga SM, et al. Identification of *Streptococcus suis* putative zoonotic virulence factors: a systematic review and genomic meta-analysis. Virulence. 2021;12(1):2787–2797. doi: 10.1080/21505594.2021.1985760

[19] Tenenbaum T, Seitz M, Schroten H, et al. Biological activities of suilysin: role in *Streptococcus suis* pathogenesis. Future Microbiol. 2016;11(7):941–954. doi: 10.2217/fmb-2016-0028

[20] Zhao T, Gussak A, van der Hee B, et al. Identification of plasminogen-binding sites in Streptococcus suis enolase that contribute to bacterial translocation across the blood-brain barrier. Front Cell Infect Microbiol. 2024;14:14. doi: 10.3389/fcimb.2024.1356628

[21] David Roy JP. *cjvr_04_141*. 2014. Available from: https://pmc.ncbi.nlm.nih.gov/articles/PMC4365706/pdf/cjvr_04_141.pdf

[22] Singh Chhatwal G, editor. Host-pathogen interactions in streptococcal diseases. In: Current topics in microbiology and immunology. Berlin, Heidelberg: Springer; 2013. p. 168. Available from: http://www.springer.com/series/82

[23] Rohmer L, Hocquet D, Miller SI. Are pathogenic bacteria just looking for food? Metabolism and microbial pathogenesis. Trends Microbiol. 2011;19(7):341–348. doi: 10.1016/j.tim.2011.04.003

[24] Molzen TE, Burghout P, Bootsma HJ, et al. Genome-wide identification of *Streptococcus pneumoniae* genes essential for bacterial replication during experimental meningitis. Infect Immun. 2011;79(1):288–297. doi: 10.1128/IAI.00631-10

[25] Gray J, Torres VVL, Goodall E, et al. Transposon mutagenesis screen in *Klebsiella pneumoniae* identifies genetic determinants required for growth in human urine and serum. Elife. 2024;12. doi: 10.7554/elife.88971

[26] Pellegrini L, Bonfio C, Chadwick J, et al. Human CNS barrier-forming organoids with cerebrospinal fluid production. Science. 2020a;369(6500):eaaz5626. doi: 10.1126/science.aaz5626

[27] Otto C, Kalantzis R, Kübler-Weller D, et al. Comprehensive analysis of the cerebrospinal fluid and serum metabolome in neurological diseases. J Neuroinflammation. 2024;21(1). doi: 10.1186/s12974-024-03218-0

[28] Nascimento FP, Macedo-Júnior SJ, Lapa-Costa FR, et al. Inosine as a tool to understand and treat central nervous system disorders: a neglected actor? Front Neurosci. 2021;15. doi: 10.3389/fnins.2021.703783

[29] van Opijnen T, Bodi KL, Camilli A. Tn-seq: high-throughput parallel sequencing for fitness and genetic interaction studies in microorganisms. Nat Methods. 2009;6(10):767–772. doi: 10.1038/nmeth.1377

[30] Arenas J, Zomer A, Harders-Westerveen J, et al. Identification of conditionally essential genes for *Streptococcus suis* infection in pigs. Virulence. 2020;11(1):446–464. doi: 10.1080/21505594.2020.1764173

[31] Juanpere-Borras M, Zhao T, Boekhorst J, et al. Genome-wide identification of conditionally essential genes supporting *Streptococcus suis* growth in serum and cerebrospinal fluid. BioRxiv. 2025. doi: 10.1101/2025.05.03.652005

[32] ATCC. *Streptococcus suis (BAA-853)*. Manassas (VA): ATCC;n.d. Available from: https://www.Atcc.Org/Products/Baa-853

[33] Van Opijnen T, Camilli A. Genome-wide fitness and genetic interactions determined by Tn-seq, a high-throughput massively parallel sequencing method for microorganisms. Curr Protoc Mol Biol. 2014;106(1). doi: 10.1002/0471142727.mb0716s106

[34] Van Der Els S, James JK, Kleerebezem M, et al. Versatile Cas9-driven subpopulation selection toolbox for *Lactococcus lactis*. Appl Environ Microbiol. 2018;84(8). doi: 10.1128/AEM.02752-17

[35] Zaccaria E, Van Baarlen P, De Greeff A, et al. Control of competence for DNA transformation in *Streptococcus suis* by genetically transferable pherotypes. PLOS ONE. 2014;9(6):e99394. doi: 10.1371/journal.pone.0099394

[36] Pellegrini L, Bonfio C, Chadwick J, et al. Human CNS barrier-forming organoids with cerebrospinal fluid production. Science. 2020b;369(6500):eaaz5626. doi: 10.1126/science.aaz5626

[37] Gussak A, Ferrando ML, Schrama M, et al. Precision genome engineering in *Streptococcus suis* based on a broad-host-range vector and CRISPR-Cas9 technology. ACS Synth Biol. 2023;12(9):2546–2560. doi: 10.1021/acssynbio.3c00110

[38] Grant CE, Bailey TL, Noble WS. FIMO: scanning for occurrences of a given motif. Bioinformatics. 2011;27(7):1017–1018. doi: 10.1093/bioinformatics/btr064

[39] Jordan S, Junker A, Helmann JD, et al. Regulation of liars-dependent gene expression in *Bacillus subtilis*: identification of inhibitor proteins, regulator binding sites, and target genes of a conserved cell envelope stress-sensing two-component system. J Bacteriol. 2006;188(14):5153–5166. doi: 10.1128/JB.00310-06

[40] DeJesus MA, Ambadipudi C, Baker R, et al. Transit - a software tool for Himar1 TnSeq analysis. PLOS Comput Biol. 2015;11(10):e1004401. doi: 10.1371/journal.pcbi.1004401

[41] Gómez-Gascón L, Luque I, Tarradas C, et al. Comparative immunosecretome analysis of prevalent *Streptococcus suis* serotypes. Comp Immunol Microbiol Infect Dis. 2018;57:55–61. doi: 10.1016/j.cimid.2018.06.006

[42] Weiße C, Dittmar D, Jakóbczak B, et al. Immunogenicity and protective efficacy of a *Streptococcus suis* vaccine composed of six conserved immunogens. Vet Res. 2021;52(1):112. doi: 10.1186/s13567-021-00981-3

[43] Franza T, Rogstam A, Thiyagarajan S, et al. Nad+ pool depletion as a signal for the Rex regulon involved in *Streptococcus agalactiae* virulence. PLOS Pathog. 2021;17(8):e1009791. doi: 10.1371/journal.ppat.1009791

[44] Jahn K, Kohler TP, Wiebe S, et al. Platelets, bacterial adhesins and the pneumococcus. Cells. 2022;11(7):1121. doi: 10.3390/cells11071121

[45] Wolf D, Kalamorz F, Wecke T, et al. In-depth profiling of the LiaR response of *Bacillus subtilis*. J Bacteriol. 2010;192(18):4680–4693. doi: 10.1128/JB.00543-10

[46] Suntharalingam P, Senadheera MD, Mair RW, et al. The LiaFSR system regulates the cell envelope stress response in *Streptococcus mutans*. J Bacteriol. 2009;191(9):2973–2984. doi: 10.1128/JB.01563-08

[47] Vega LA, Sansón-Iglesias M, Mukherjee P, et al. Liar-dependent gene expression contributes to antimicrobial responses in group A*Streptococcus*. Antimicrob Agents Chemother. 2024;68(12). doi: 10.1128/aac.00496-24

[48] Sanson MA, Vega LA, Shah B, et al. The LiaFSR transcriptome reveals an interconnected regulatory network in group A *Streptococcus*. Infect Immun. 2021;89(11). doi: 10.1128/IAI.00215-21

[49] Abdullah MR, Batuecas MT, Jennert F, et al. Crystal structure and pathophysiological role of the pneumococcal nucleoside-binding protein PnrA. J Mol Biol. 2021;433(2):166723. doi: 10.1016/j.jmb.2020.11.022

[50] Deka RK, Brautigam CA, Yang XF, et al. The PnrA (Tp0319; TmpC) lipoprotein represents a new family of bacterial purine nucleoside receptor encoded within an ATP-binding cassette (ABC)-like operon in *Treponema pallidum*. J Biol Chem. 2006;281(12):8072–8081. doi: 10.1074/jbc.M511405200

[51] Bleuzé M, Lavoie JP, Bédard C, et al. Encapsulated *Streptococcus suis* impairs optimal neutrophil functions which are not rescued by priming with colony-stimulating factors. PLOS ONE. 2024;19(1):e0296844. doi: 10.1371/journal.pone.0296844

[52] Bourgeois J, Camilli A. High-throughput mutant screening via transposon sequencing. Cold Spring Harb Protoc. 2023;2023(10):707–709. doi: 10.1101/pdb.top107867

[53] Rosconi F, Rudmann E, Li J, et al. A bacterial pan-genome makes gene essentiality strain-dependent and evolvable. Nat Microbiol. 2022;7(10):1580–1592. doi: 10.1038/s41564-022-01208-7

[54] Dresen M, Schaaf D, Arenas J, et al. *Streptococcus suis* TrpX is part of a tryptophan uptake system, and its expression is regulated by a T-box regulatory element. Sci Rep. 2022;12(1). doi: 10.1038/s41598-022-18227-3

[55] Le Breton Y, Mistry P, Valdes KM, et al. Genome-wide identification of genes required for fitness of group A *Streptococcus* in human blood. Infect Immun. 2013;81(3):862–875. doi: 10.1128/IAI.00837-12

[56] Saxena S, Khan N, Dehinwal R, et al. Conserved surface accessible nucleoside ABC transporter component SP0845 is essential for pneumococcal virulence and confers protection in vivo. PLOS ONE. 2015;10(2):e0118154. doi: 10.1371/journal.pone.0118154

[57] Jain S, Sutchu S, Rosa PA, et al. Borrelia burgdorferi harbors a transport system essential for purine salvage and mammalian infection. Infect Immun. 2012;80(9):3086–93. doi: 10.1128/IAI.00514-12.

[58] Li L, Abdelhady W, Donegan NP, et al. Role of purine biosynthesis in persistent methicillin-resistant *Staphylococcus aureus* infection. J Infect Dis. 2018;218(9):1367–1377. doi: 10.1093/infdis/jiy340

[59] Mantena RKR, Wijburg OLC, Vindurampulle C, et al. Reactive oxygen species are the major antibacterials against *Salmonella typhimurium* purine auxotrophs in the phagosome of RAW 264.7 cells. Cell Microbiol. 2008;10(5):1058–1073. doi: 10.1111/j.1462-5822.2007.01105.x

[60] Samant S, Lee H, Ghassemi M, et al. Nucleotide biosynthesis is critical for growth of bacteria in human blood. PLoS Pathog. 2008;4(2):e37. doi: 10.1371/journal.ppat.0040037

[61] Schauer K, Geginat G, Liang C, et al. Deciphering the intracellular metabolism of *Listeria monocytogenes* by mutant screening and modelling. BMC Genomics. 2010;11(1). doi: 10.1186/1471-2164-11-573

[62] Lan L, Cheng A, Dunman PM, et al. Golden pigment production and virulence gene expression are affected by metabolisms in *Staphylococcus aureus*. J Bacteriol. 2010;192(12):3068–3077. doi: 10.1128/JB.00928-09

[63] Mei JM, Nourbakhsh F, Ford CW, et al. Identification of *Staphylococcus aureus* virulence genes in a murine model of bacteraemia using signature-tagged mutagenesis. Mol Microbiol. 1997;26(2):399–407. doi: 10.1046/j.1365-2958.1997.5911966.x

[64] Valentino MD, Foulston L, Sadaka A, et al. Genes contributing to *Staphylococcus aureus* fitness in abscess- and infection-related ecologies. MBio. 2014;5(5). doi: 10.1128/mBio.01729-14

[65] Wilde AD, Snyder DJ, Putnam NE, et al. Bacterial hypoxic responses revealed as critical determinants of the host-pathogen outcome by TnSeq analysis of *Staphylococcus aureus* invasive infection. PLoS Pathog. 2015;11(12):e1005341. doi: 10.1371/journal.ppat.1005341

[66] Goncheva MI, Chin D, Heinrichs DE. Nucleotide biosynthesis: the base of bacterial pathogenesis. Trends Microbiol. 2022;30(8):793–804. doi: 10.1016/j.tim.2021.12.007

[67] Shaffer CL, Zhang EW, Dudley AG, et al. Purine biosynthesis metabolically constrains intracellular survival of uropathogenic *Escherichia coli*. Infect Immun. 2017;85(1). doi: 10.1128/IAI.00471-16

[68] Huemer M, Mairpady Shambat S, Bergada-Pijuan J, et al. Molecular reprogramming and phenotype switching in *Staphylococcus aureus* lead to high antibiotic persistence and affect therapy success. Proc Natl Acad Sci. 2021;118(7). doi: 10.1073/pnas.2014920118

[69] Liedel C, Rieckmann K, Baums CG. A critical review on experimental *Streptococcus suis* infection in pigs with a focus on clinical monitoring and refinement strategies. BMC Vet Res. 2023;19(1). doi: 10.1186/s12917-023-03735-9

[70] Juanpere-Borras M. Raw and processed data for nanopore-based tn-seq analysis. *Prjeb89170*. European Nucleotide Archive (ENA); 2025. Available from: https://www.ebi.ac.uk/ena/browser/view/PRJEB89170

[71] van Baarlen P, Juanpere Borras M. Genome-wide identification of conditionally essential genes supporting *Streptococcus suis* growth in serum and cerebrospinal fluid– supplementary dataset, version 1. 4tu. researchdata. 2025. doi: 10.4121/ace99cb5-0414-4a91-9aa8-72c0d8c47381.v1